Coupled Vibration Analysis of a Beam-Arch Composite Continuous Rigid Structure with Parallel Traffic Flow

Rui Han [1,a]

[1] Chang'an University, School of Highway, Shaanxi, Xi'an 710064, China

[a] e-mail address: 1065416661@qq.com

Abstract. To investigate the structural dynamic characteristics of a beam-arch composite continuous rigid structure bridge under the action of parallel moving loads on a multi-lane highway, a joint simulation analysis program based on Easy Language and ANSYS was developed. This study was conducted using a six-span beam-arch composite continuous rigid structure bridge located in Shaanxi Province as the reference project. The research focused on the most adverse dynamic coupled responses of the main beam midspan, arch crown, and suspension rods caused by double-axle cars, double-axle trucks, and three-axle trucks on a single-direction three-lane road surface.

The research results indicate that for single-direction traffic flow with multiple lanes and single vehicles, as the number of lanes increases, the peak dynamic responses at various cross-sections also increase. Specifically, transitioning from a single-lane condition to a double-lane condition results in a 117% increase in the peak dynamic displacement at the main beam midspan, a 38.1% increase in the peak dynamic bending moment at the main beam midspan, a 54% increase in the peak dynamic displacement at the arch crown, a 41% increase in the peak dynamic bending moment at the arch crown, a 59.7% increase in the peak dynamic tension force in the longest suspension rod, and a 64.2% increase in the peak dynamic tension force in the shortest suspension rod. When transitioning from a double-lane condition to a three-lane condition, there is a 1.07% increase in the peak dynamic displacement at the main beam midspan, a 39.5% increase in the peak dynamic bending moment at the main beam midspan, a 1.97% increase in the peak dynamic displacement at the arch crown, a 21.80% increase in the peak dynamic bending moment at the arch crown, a 1.16% increase in the peak dynamic tension force in the longest suspension rod, and a 15.22% increase in the peak dynamic tension force in the shortest suspension rod.

Regarding the dynamic amplification factors, the dynamic displacement amplification factors at the main span midspan and arch crown, as well as the dynamic tension force amplification factors in the longest suspension rods at each span, decrease as the number of lanes increases. Specifically, transitioning from a single-lane condition to a double-lane condition results in a 12.92% decrease in the dynamic displacement amplification factor at the main beam midspan and a 15.95% decrease in the dynamic displacement amplification factor at the arch crown. When transitioning from a double-lane condition to a three-lane condition, there is a 0.97% decrease in the dynamic displacement amplification factor at the main beam midspan, and the dynamic displacement amplification factor at the arch crown changes from 1.499mm to 1.502mm, showing a minor change. The dynamic bending moment amplification factors at the main span midspan and the dynamic tension force amplification factors in the shortest suspension rods at each span are not linearly correlated with the number of lanes, while the dynamic bending moment at the arch crown increases with an increase in the number of lanes.

For the continuous rigid structure of the beam-arch composite system, the dynamic amplification factors vary for different bridge components. The maximum dynamic displacement amplification factor at the main span midspan is 1.452, the maximum dynamic bending moment amplification factor at the main span midspan is 1.327, the maximum dynamic displacement amplification factor at the arch crown is 1.773, the maximum dynamic bending moment amplification factor at the arch crown is 3.137, the maximum dynamic tension force amplification factor in the longest suspension rod is 1.602, and the maximum dynamic tension force amplification factor in the shortest suspension rod is 1.265. For this bridge, the dynamic amplification factors specified by relevant standards are 1.05, which is less than the calculated results in this study. Therefore, the current standards for dynamic amplification factors for this type of bridge are not

conservative, and it is not appropriate to use a uniform maximum dynamic amplification factor for the entire bridge. In setting standards for dynamic amplification factors, separate values should be established for each bridge component, and this should be taken into consideration in the design, maintenance, and reinforcement of such bridges in the future.

Keywords: Bridge Engineering; Beam-Arch Composite System Bridge; Vehicle-Bridge Coupling; Structural Dynamic Response.

1. Introduction

As bridge spans continue to increase, bridge designs evolve, and vehicles advance towards higher speeds and heavier loads, the issue of vehicle-bridge coupled vibration becomes increasingly prominent. Currently, there is significant research on vehicle-bridge coupled vibration in the context of simply supported beam bridges [1], continuous beam bridges [2-3], and cable-stayed bridges [4-5]. Researchers such as He Xuanbo [6] conducted a vehicle-bridge coupled vibration analysis on a medium-span arch bridge, including fatigue life analysis and evaluation of suspension rods. Han Zhiqiang and Xie Gang [3], using custom programs, analyzed vehicle-bridge coupled vibration on a large-span continuous beam bridge. Wang Xiaoyong [7] conducted vehicle-bridge coupled vibration analysis on a continuous rigid frame bridge from a real-world project and evaluated ride comfort. Yao Dunrong and Deng Nianchun [8], based on vehicle-bridge coupled vibration theory and using the multibody dynamics software Universal Mechanism (UM), analyzed factors such as road roughness, traffic spacing, and bridge structural damping. Lu Sun and Xingzhuang Zhao [9] proposed an elastic method to discretize the beam into lumped masses in three dimensions, improving computational accuracy and efficiency compared to traditional finite element methods. Charikleia D. Stoura [10] introduced a dynamic partitioning method (DPM) to address vehicle-bridge interaction problems by introducing auxiliary contact bodies between vehicles and bridge systems and employing a component-wise Lagrange multiplier method to avoid numerical challenges encountered in differential-algebraic equation (DAE) approaches. Junhee Kim proposed a wireless monitoring system that installs wireless sensors on both the bridge and moving vehicles to record the dynamic interaction between the bridge and the vehicles [11-12].

The beam-arch composite system bridge is a special type of bridge that represents an evolution of traditional arch bridges, combining the advantages of both beam and arch bridges. This combination not only finds wide application in highway bridges but is also increasingly favored for its aesthetic appeal in urban bridge construction [13]. Existing research has mainly focused on single-lane, single-vehicle parameter discussions for traditional beam bridges or simple arch bridges, with limited studies on the coupled vibration analysis of new beam-arch composite system bridges under complex multi-lane, multi-vehicle conditions. While the probability of multiple lanes with parallel traffic flow on in-service bridges may be relatively low, concentrated loading due to such scenarios can be more structurally disadvantageous compared to random traffic, potentially leading to extreme adverse conditions with compounded dynamic responses.

Therefore, this paper specifically targets beam-arch composite system bridges and analyzes the vehicle-bridge coupled vibration response patterns of the main beam dynamic displacement and bending moments, arch crown bending moments, and suspension rod tension forces under multi-lane, multi-vehicle conditions with one-way traffic, considering variations in vehicle speed, lane position, and vehicle count. This research aims to provide insights for developing impact coefficients for similar beam-arch composite systems and making operational and maintenance decisions.

2. Vehicle-Bridge Model

2.1 Bridge Profile

This article is based on an engineering project in Shaanxi Province, where a beam-arch composite continuous rigid structure bridge is used as the foundation. The span combination consists of 90m + 170m × 4 + 90m, totaling 860m. The main bridge box girder is constructed with prestressed concrete and features a variable cross-section design. The total width of the bridge is 41.6m. It has a single-box, single-chamber cross-section, with a beam height of 9.5m at the root and 3.8m at the midspan. The thickness of the bottom slab gradually varies from 35cm at the midspan to 90cm at the root (as shown in Figures 1.1 to 1.2). This section is located in a traffic hub area with high daily traffic flow. The bridge is designed with six lanes in both directions and serves as a primary highway with municipal functions.

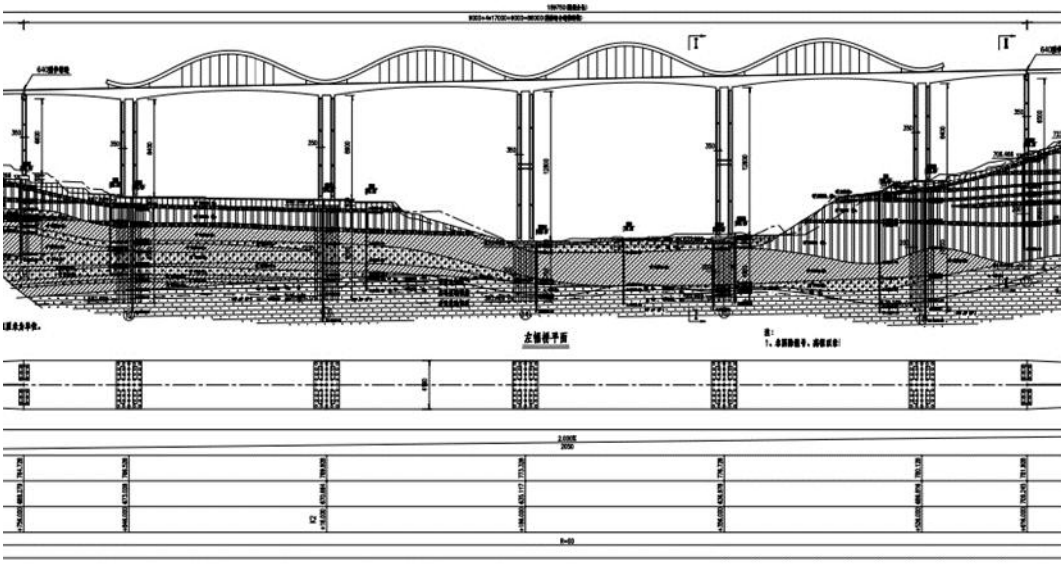

Fig 1 Bridge general arrangement drawing

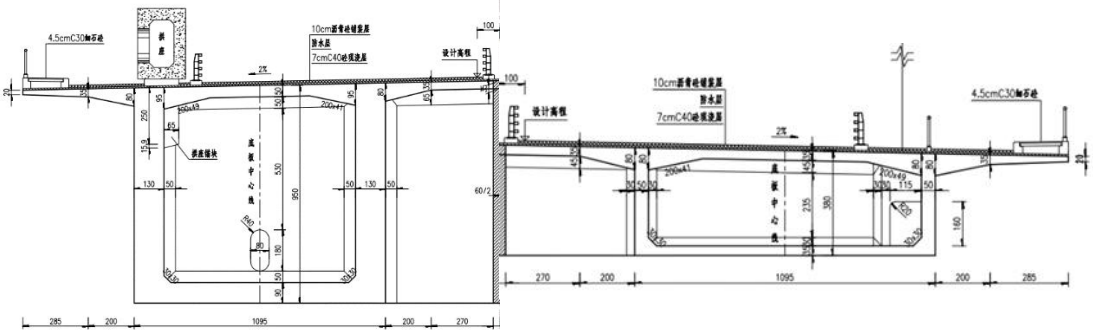

Fig 2 Bridge pier and mid-span cross-section drawing

2.2 Bridge Finite Element Model

A finite element model of the bridge is established using the general-purpose finite element software ANSYS. Both the main beam and the main arch are modeled using the BEAM188 elements available in ANSYS. The suspension rods are modeled using the LINK10 elements, and the permanent load for the second phase is modeled using the MASS21 elements. Since the main beam of this bridge has a variable cross-section box girder, it is necessary to define sections at adjacent nodes. Due to the relatively fine mesh division of the bridge structure, defining adjacent sections manually would be a time-consuming task. Therefore, when writing ANSYS APDL command streams, the sectype, secdata, secwrite, and secoffset command groups are used to define sections at adjacent nodes with section numbers i and t=i+1. These commands are combined with

do loop commands to efficiently and accurately generate continuous variable cross-sections, facilitating the precise modeling of the main beam.

Rigid connections are implemented between the main beam and the main pier. The connections between the suspension rods and the main beam, as well as the main arch, are established using the CP command streams to couple nodes. Additionally, each suspension rod is assigned independent parameter arrays and real constants, which facilitates adjusting initial tension and later data retrieval. The finite element model is illustrated in Figure 3.

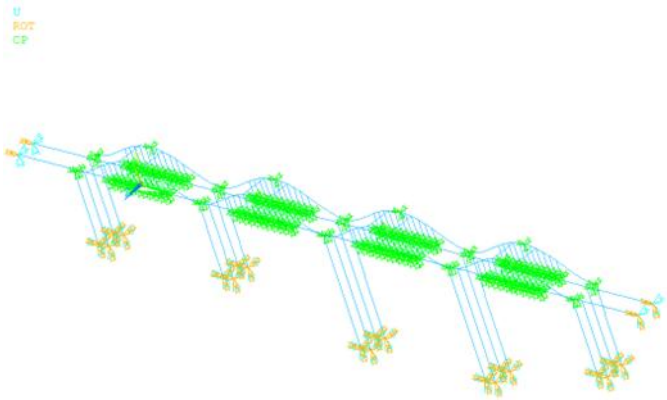

Fig 3 Bridge finite element model drawing

2.3 Vehicle Model

The vehicle model is simulated using ANSYS's mass elements (such as MASS21) to represent the vehicle body mass and wheel masses, and spring-damper elements (COMBIN14) to simulate the vehicle suspension and tires. This approach takes into account the three-dimensional vibration response characteristics of the vehicle body, suspension, and tires, allowing it to accurately reflect the vehicle's vibration characteristics while being technically feasible. By analyzing relevant literature on commonly used vehicle models for highway bridges and conducting surveys of actual traffic flow at the project site, a decision was made to select spatial two-axle and three-axle vehicle models to accurately simulate vehicles under real-world conditions. Figure 4 provides a schematic diagram and parameter description of the spatial two-axle and three-axle vehicle models used in the vehicle-bridge coupled vibration analysis program.

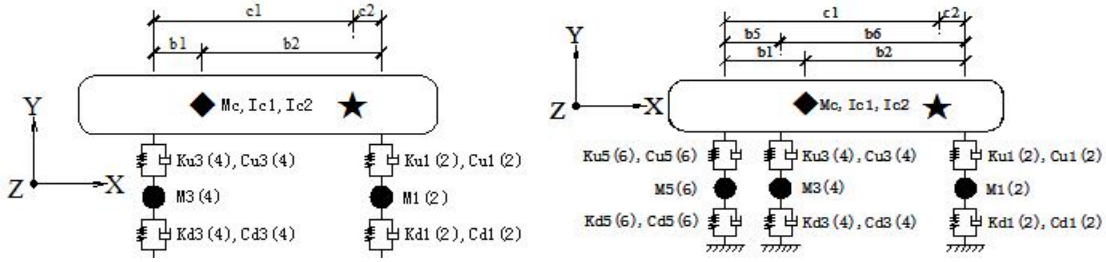

Fig 4 The seven-degree-of-freedom spatial double-axle vehicle model and The nine-degree-of-freedom spatial triple-axle vehicle model

3. Vehicle-Bridge Coupled Vibration Analysis

3.1 Worst-Case Vehicle Speed Analysis

When moving vehicles traverse a bridge structure, different driving speeds can result in varying impact forces on the bridge structure. This leads to different dynamic responses of the bridge structure and dynamic amplification factors. In order to determine the parameters of each vehicle under multi-vehicle scenarios to meet the worst-case conditions, it is necessary to control variables in single-vehicle scenarios in order to analyze and obtain the values of each parameter.

Considering the factors mentioned above, it is first necessary to identify which of the three vehicle types induces the maximum dynamic response and dynamic amplification factors in the bridge. Subsequently, an analysis with variable parameters will be performed using the vehicle type that produces these maximum values. Below, calculations will be conducted for the individual loading of the three vehicle types on the main beams #1 and #2, focusing on dynamic displacement and dynamic bending moments.

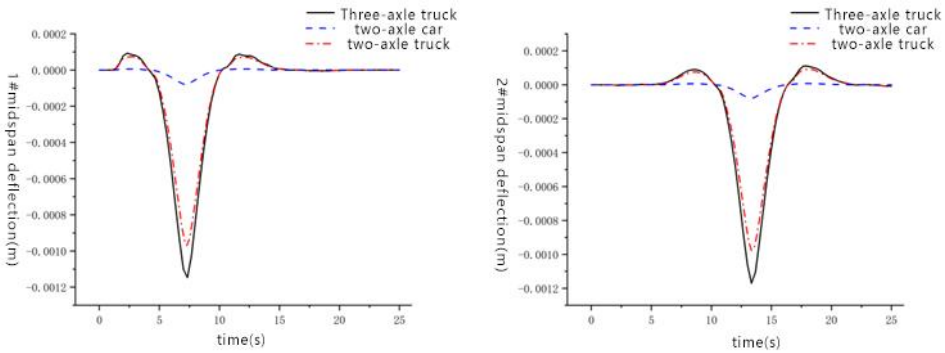

Figure 5 the peak dynamic displacements at the midspan of main beams #1 and #2 are presented for each vehicle type and loading condition

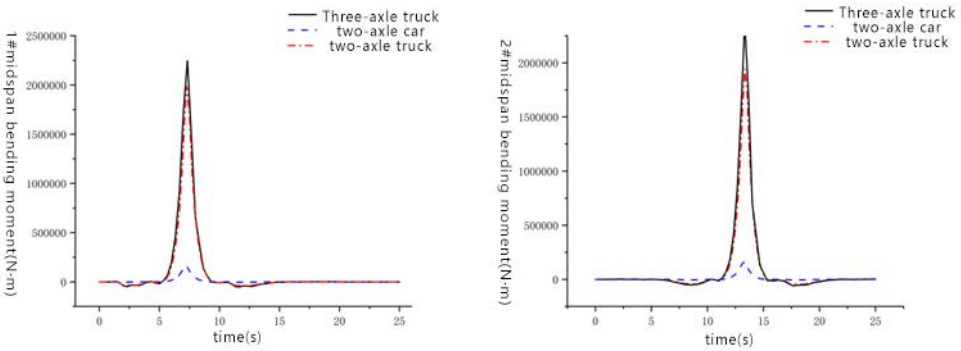

Figure 6 The peak dynamic bending moments at the midspan of main beams #1 and #2 under different vehicle types and loading conditions

From the calculation results in Figures 5 and 6, it is evident that for single-vehicle loading scenarios, the three-axle heavy vehicle imposes a more adverse dynamic response on the bridge. Therefore, for the parameter analysis calculations, the three-axle heavy vehicle is selected as the vehicle model.

Considering that the chosen vehicle model is a 33-ton three-axle truck, as per the "Regulations on the Implementation of the Road Traffic Safety Law of the People's Republic of China," this type of vehicle should travel in the rightmost lane with a speed limit ranging from 60 km/h to 100 km/h. Therefore, when studying the impact of vehicle speed on the dynamic response of the bridge

structure and dynamic amplification factors, vehicle speeds ranging from 60 km/h to 100 km/h are selected with a 10 km/h increment. When selecting the analysis sections, midspan sections of the main beams and the arch crown sections for each span are chosen to analyze their dynamic displacements and dynamic amplification factors.

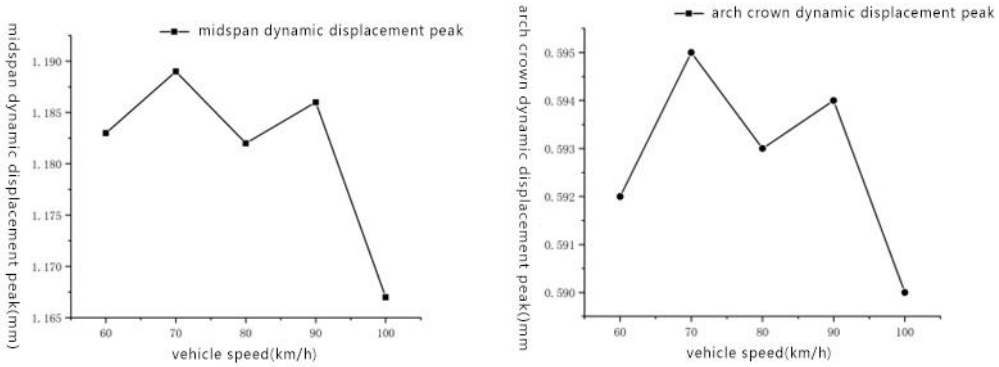

Fig 7 Peak dynamic displacement of #1 main beam midspan and arch crown under various vehicle speed conditions

The calculation results from Figure 5 reveal that for the 33-ton heavy vehicle, the dynamic displacement and its dynamic amplification factors at the midspan and arch crown of the main beams are highly sensitive to a speed of 70 km/h. Therefore, when performing calculations for multi-vehicle parallel bridge crossing scenarios to assess the worst-case vehicle-bridge coupled vibration response, a vehicle speed of 70 km/h is selected.

3.2 Load Case Calculation

The bridge has six lanes divided into three lanes on each side, making it a double-lane, six-lane bridge. The lane closest to the centerline of the bridge is designated as the #1 lane, followed by the #2 lane, and then the #3 lane as we move outward. Under one-way traffic conditions, the multiple lane combinations can be grouped into #1+#2, #1+#3, #2+#3, and #1+#2+#3 based on a full permutation. Additionally, following traffic rules, the #1 lane is loaded with two-axle cars, the #2 lane with two-axle heavy vehicles, and the #3 lane with three-axle heavy vehicles.

Considering the dynamic responses and dynamic amplification factors calculated for the different vehicle types in section 2.1.1, it's evident that the dynamic response of the three-axle heavy vehicle is significantly greater than the first two. Therefore, when analyzing the impact of the number of lanes loaded on the vehicle-bridge coupling effects, to simultaneously meet the worst-case conditions and the actual operation of vehicles, the single-lane scenario is taken as #3, the double-lane scenario builds upon this with a more adverse #2+#3 combination, and the triple-lane scenario selects #1+#2+#3. This is done to analyze the effects of vehicle-bridge coupling under the simultaneous loading of multiple lanes and the number of loaded lanes.

From section 2.1, it was determined that the vehicle traveling speed is set at 70 km/h.

3.2.1 Single-Lane Scenario Calculation

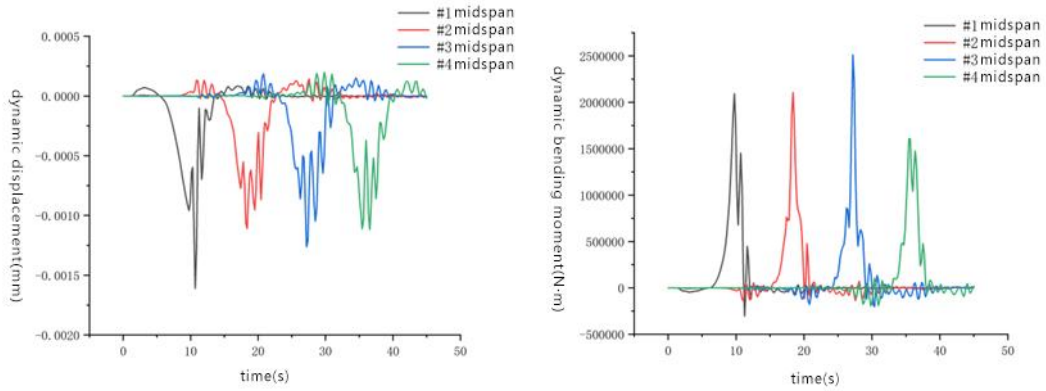

Fig 9 Time history curves of dynamic displacement and bending moment at each span of the main beam under single-lane working condition

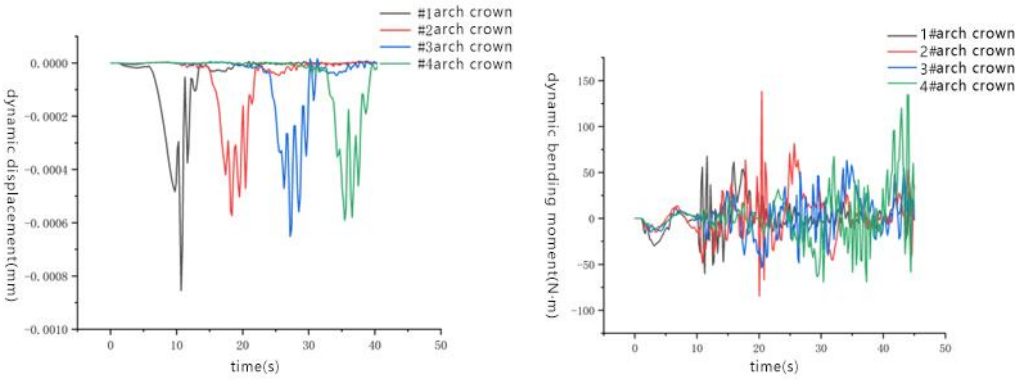

Fig 10 Time history curves of dynamic displacement and bending moment at the crown of each arch under single-lane working condition

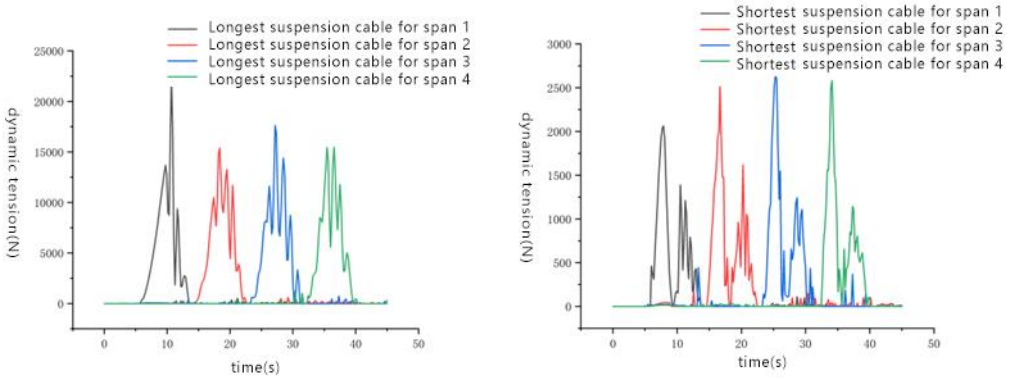

Fig 11 Time history curves of dynamic tension force in the longest and shortest hanger rods of each arch under single-lane working condition

Based on the calculations above, it can be observed that in the single-lane bridge crossing scenario, the peak dynamic displacement response for the main beam section reaches a maximum of 1.161 mm at the #1 span, and the dynamic amplification factor also peaks at 1.658. Regarding the dynamic bending moment response for the main beam section, it reaches a maximum of 2511.44 kN·m at the #3 span, with a corresponding dynamic amplification factor peaking at 1.189. For the dynamic displacement response of the main arch section, it is similar to that of the main beam

midspan, reaching a maximum of 0.855 mm at the #1 span, with a dynamic amplification factor peaking at 1.773. As for the dynamic bending moment response for the main arch section, it reaches a maximum of 151.458 N·m at the #4 arch crown, while the dynamic amplification factor peaks at the #2 arch crown, reaching 3.137. The longest suspension rod experiences the highest dynamic tension response, with a peak tension of 22324.4 N at the longest suspension rod of the #1 span, and its dynamic amplification factor also reaches a peak of 1.602. The shortest suspension rod experiences the highest dynamic tension response, with a peak tension of 2640.62 N at the shortest suspension rod of the #3 span, and its dynamic amplification factor also reaches a peak of 1.222.

Considering the overall results, it is often observed that the dynamic responses for the main beam midspan and the main arch crown occur in the same span. Except for the dynamic bending moment response of the main arch, which does not peak in the same span as its dynamic amplification factor, all other responses for various sections peak in the same span as their corresponding dynamic amplification factors. When comparing the dynamic amplification factors of various bridge components, it is consistent with the single-lane scenario, with an overall trend of arch > beam > suspension rod.

3.2.2 Double-Lane Scenario Calculation

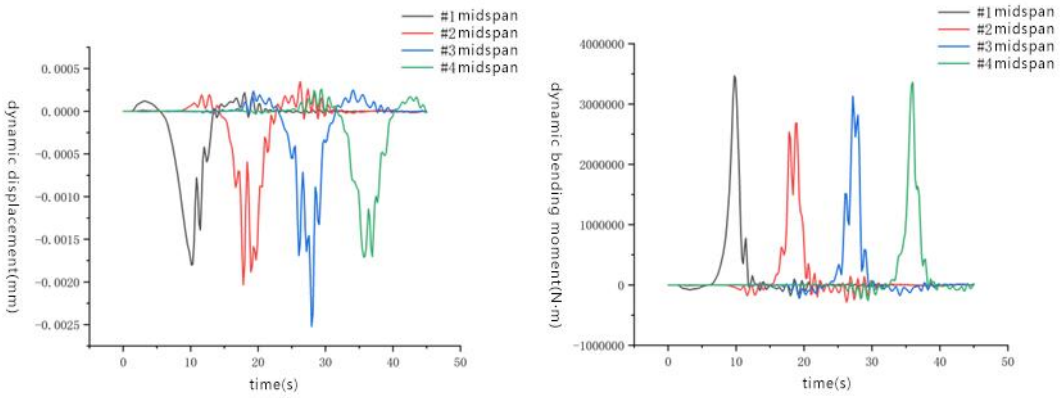

Fig 12 Time history curves of dynamic displacement and bending moment at each span of the main beam under double-lane working condition

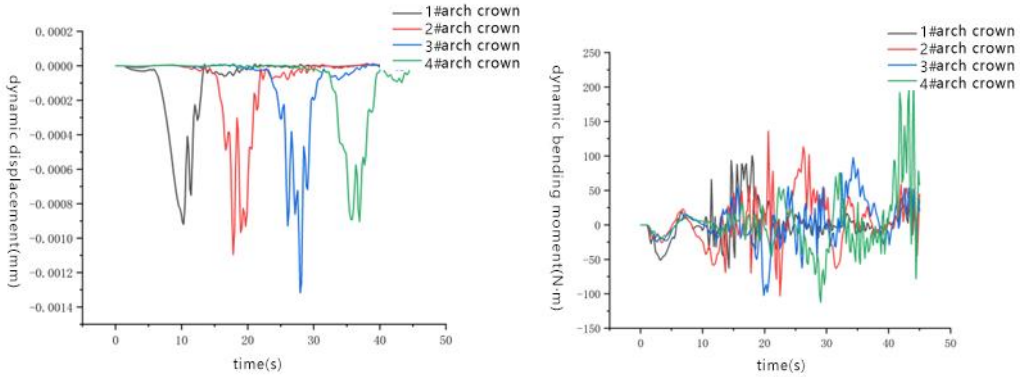

Fig 13 Time history curves of dynamic displacement and bending moment at the crown of each arch under double-lane working condition

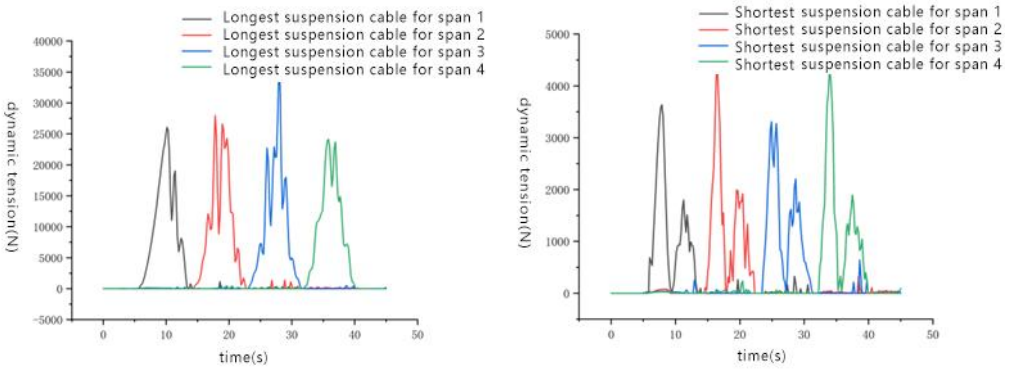

Fig 14 Time history curves of dynamic tension force in the longest and shortest hanger rods of each arch under double-lane working condition

Based on the calculations above, it can be observed that in the double-lane bridge crossing scenario, the peak dynamic displacement response for the main beam section reaches a maximum of 2.522 mm at the #3 span, and the dynamic amplification factor also peaks at 1.452. Regarding the dynamic bending moment response for the main beam section, it reaches a maximum of 3470.02 kN·m at the #1 span, with a corresponding dynamic amplification factor peaking at 0.973. For the dynamic displacement response of the main arch section, it is similar to that of the main beam midspan, reaching a maximum of 1.317 mm at the #3 span, with a dynamic amplification factor peaking at 1.499. As for the dynamic bending moment response for the main arch section, it reaches a maximum of 213.083 N·m at the #4 arch crown, with a corresponding dynamic amplification factor peaking at 1.877. The longest suspension rod experiences the highest dynamic tension response, with a peak tension of 35628.8 N at the longest suspension rod of the #3 span, and its dynamic amplification factor also reaches a peak of 1.430. The shortest suspension rod experiences the highest dynamic tension response, with a peak tension of 4334.59 N at the shortest suspension rod of the #2 span, and its dynamic amplification factor also reaches a peak of 1.169.

Considering the overall results, similar to the single-lane scenario, it is often observed that the dynamic responses for the main beam midspan and the main arch crown occur in the same span. In the double-lane scenario, for each section, the responses and their corresponding dynamic amplification factors peak in the same span. When comparing the dynamic amplification factors of various bridge components, it is consistent with the single-lane scenario, with an overall trend of arch > beam > suspension rod.

3.2.3 Three-Lane Scenario Calculation

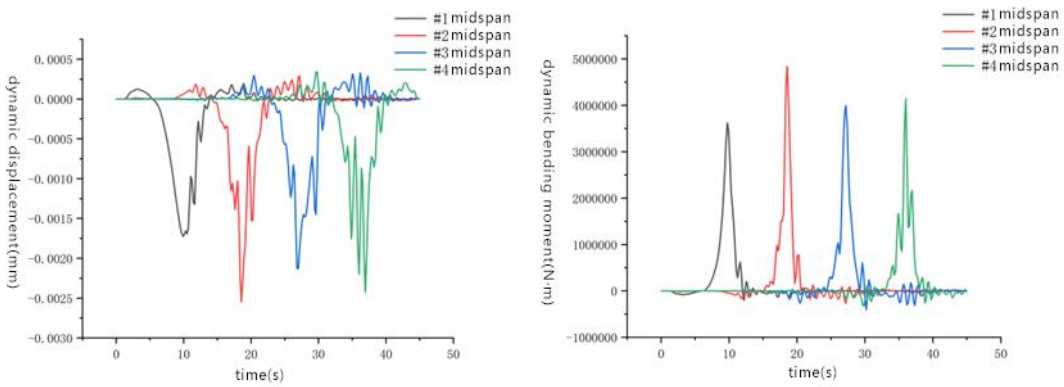

Fig 15 Time history curves of dynamic displacement and bending moment at each span of the main beam under triple-lane working condition

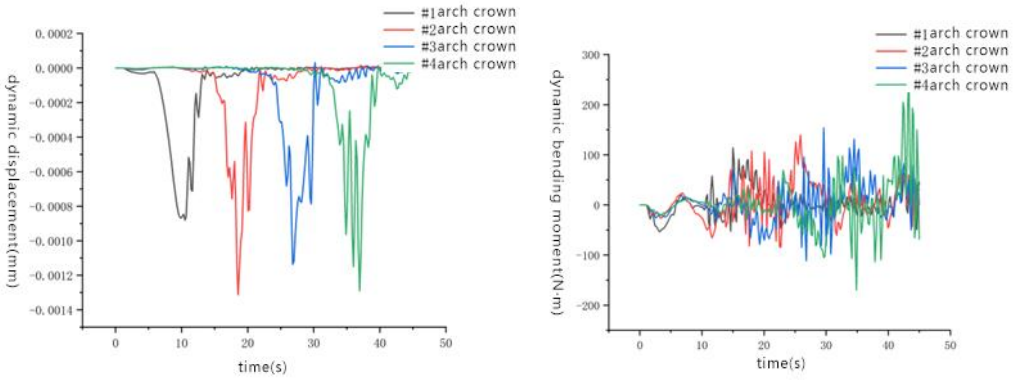

Fig 16 Time history curves of dynamic displacement and bending moment at the crown of each arch under triple-lane working condition

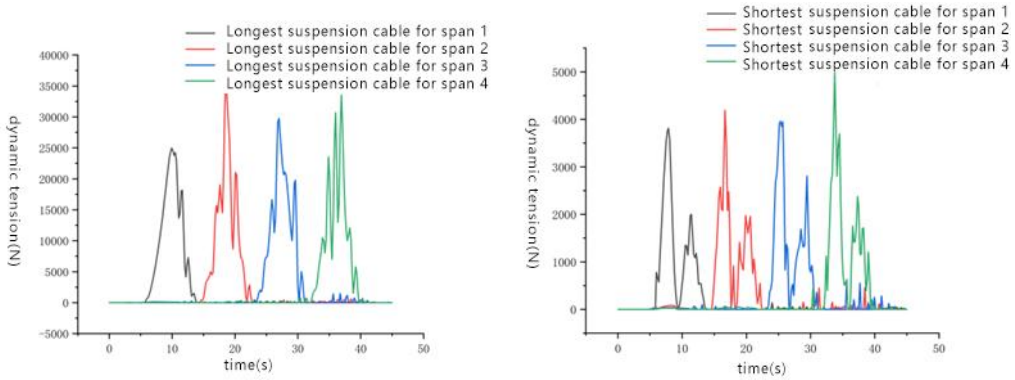

Fig 17 Time history curves of dynamic tension force in the longest and shortest hanger rods of each arch under triple-lane working condition

Based on the calculations above, it can be observed that in the three-lane bridge crossing scenario, the peak dynamic displacement response for the main beam section reaches a maximum of 2.549 mm at the #2 span, and the dynamic amplification factor also peaks at 1.438. Regarding the dynamic bending moment response for the main beam section, it reaches a maximum of 4841.35 kN·m at the #2 span, with a corresponding dynamic amplification factor peaking at 1.327. For the dynamic displacement response of the main arch section, it is similar to that of the main beam midspan, reaching a maximum of 1.343 mm at the #2 span, with a dynamic amplification factor peaking at 1.502. As for the dynamic bending moment response for the main arch section, it reaches a maximum of 259.527 N·m at the #4 arch crown, while the dynamic amplification factor peaks at the #4 arch crown, reaching 2.211. The longest suspension rod experiences the highest dynamic tension response, with a peak tension of 36042.3 N at the longest suspension rod of the #2 span, and its dynamic amplification factor also reaches a peak of 1.406. The shortest suspension rod experiences the highest dynamic tension response, with a peak tension of 4993.96 N at the shortest suspension rod of the #4 span, and its dynamic amplification factor also reaches a peak of 1.265.

Considering the overall results, it is often observed that the dynamic responses for the main beam midspan and the main arch crown occur in the same span. In the three-lane scenario, all responses for various sections peak in the same span as their corresponding dynamic amplification factors. When comparing the dynamic amplification factors of various bridge components, it is consistent with the single-lane and double-lane scenarios, with an overall trend of arch > beam > suspension rod.

3.2.4 The analysis of the impact of lane quantity on vehicle-bridge coupling effects and dynamic amplification factors

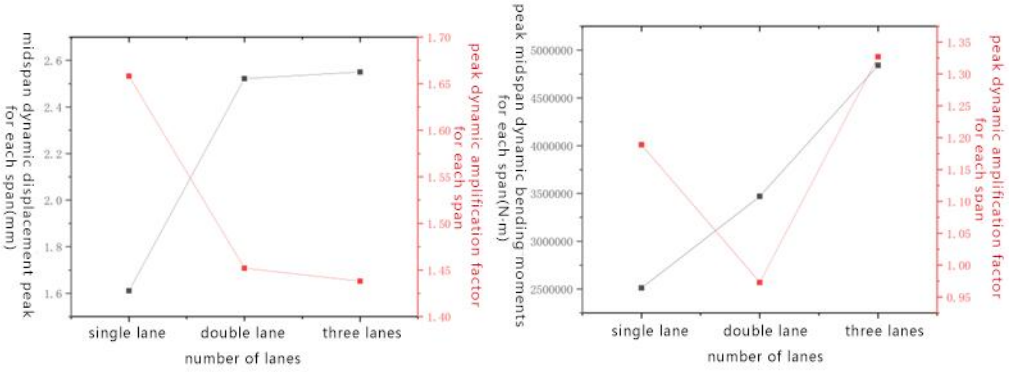

Fig 18 Peak dynamic displacement, bending moment, and corresponding dynamic amplification factor at each span

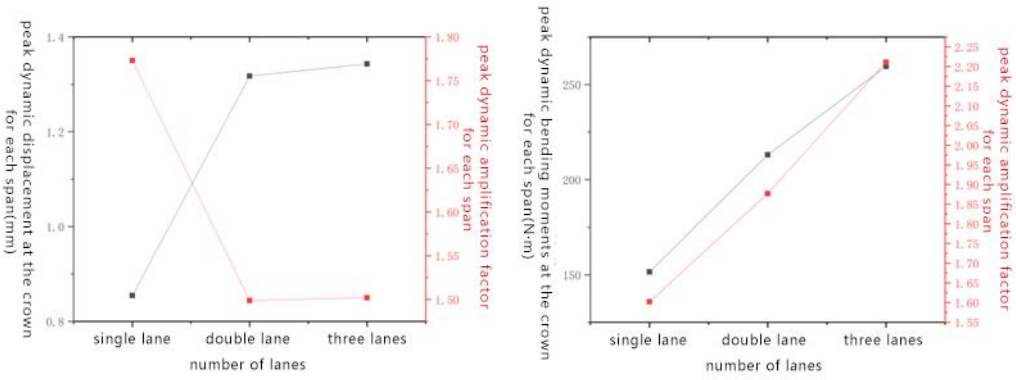

Fig 19 Peak dynamic displacement, bending moment, and corresponding dynamic amplification factor at the crown of each arch

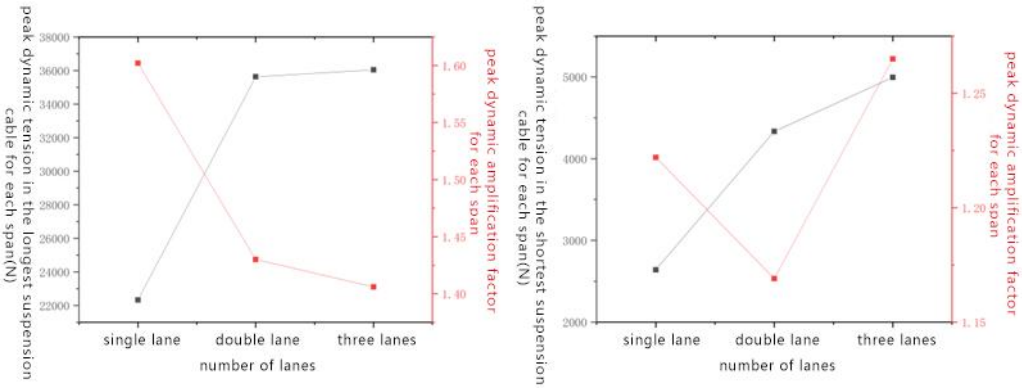

Fig 20 Peak dynamic tension force in the longest and shortest hanger rods of each span and corresponding dynamic amplification factor

From Figures 18-20, it can be observed that as the number of lanes increases, the peak dynamic displacements and moments at various spans of the bridge, as well as the peak dynamic displacements and moments at various arch crowns, and the peak dynamic tensions in the longest and shortest suspender rods, all increase. Specifically, when transitioning from a single-lane scenario to a double-lane scenario, the following changes were observed: The peak dynamic displacement at the main beam midspan increased from 1.161mm to 2.522mm, a 117% increase.

The peak dynamic moment at the main beam midspan increased from 2511.44KN·m to 3470.02KN·m, a 38.1% increase. The peak dynamic displacement at the main arch crown increased from 0.855mm to 1.317mm, a 54% increase. The peak dynamic moment at the main arch crown increased from 151.458KN·m to 213.083KN·m, a 41% increase. The peak dynamic tension in the longest suspender rod increased from 22324.4 to 35628.8, a 59.7% increase. The peak dynamic tension in the shortest suspender rod increased from 2640.62 to 4334.59, a 64.2% increase.

When transitioning from a double-lane scenario to a triple-lane scenario, the changes were as follows: The peak dynamic displacement at the main beam midspan increased from 2.522mm to 2.549mm, a 1.07% increase. The peak dynamic moment at the main beam midspan increased from 3470.02KN·m to 4841.35KN·m, a 39.5% increase. The peak dynamic displacement at the main arch crown increased from 1.317mm to 1.343mm, a 1.97% increase. The peak dynamic moment at the main arch crown increased from 213.083KN·m to 259.527KN·m, a 21.80% increase. The peak dynamic tension in the longest suspender rod increased from 35628.8 to 36042.3, a 1.16% increase. The peak dynamic tension in the shortest suspender rod increased from 4334.59 to 4993.96, a 15.22% increase.

It can be concluded that the increase from a single-lane to a double-lane scenario results in a much larger change compared to the transition from a double-lane to a triple-lane scenario. This is because the weights of the vehicles in the 3rd lane (three-axle heavy truck) and 2nd lane (two-axle heavy truck) are significantly greater than those in the 1st lane (two-axle car). As the scenarios transition from #3 to #2+#3 and then to #1+#2+#3, the total load increases, but the increase in load from #3 to #2+#3 is much larger than the increase from #2+#3 to #1+#2+#3. This aligns with the earlier conclusion that the main reason for the increase in dynamic responses at various sections is the increase in total load with the number of lanes.

In terms of the dynamic amplification factor, overall, as the number of lanes increases, the dynamic amplification factors for midspan and arch crown dynamic displacements actually decrease. Specifically, when transitioning from a single-lane scenario to a double-lane scenario, the following changes were observed: The dynamic amplification factor for midspan dynamic displacement of the main beam decreased from 1.658 to 1.452, a decrease of 12.92%. The dynamic amplification factor for arch crown dynamic displacement of the main arch decreased from 1.773 to 1.499, a decrease of 15.95%.

When transitioning from a double-lane scenario to a triple-lane scenario, the changes were as follows: The dynamic amplification factor for midspan dynamic displacement of the main beam decreased from 1.452 to 1.438, a decrease of 0.97%. The dynamic amplification factor for arch crown dynamic displacement of the main arch changed slightly from 1.499 to 1.502.

For the arch crown dynamic moment dynamic amplification factor, it generally shows an increasing trend with an increasing number of lanes. However, the dynamic amplification factor for midspan moment exhibits a fluctuating trend and does not show a linear correlation.

Regarding the dynamic tension dynamic amplification factor for the longest suspender rod, it decreases as the number of lanes increases. Specifically, when transitioning from a single-lane scenario to a double-lane scenario, the dynamic amplification factor for the longest suspender rod decreased from 1.602 to 1.430, a decrease of 10.78%. When transitioning from a double-lane scenario to a triple-lane scenario, the dynamic amplification factor for the longest suspender rod decreased from 1.430 to 1.406, a decrease of 1.68%. In contrast, the dynamic amplification factor for the shortest suspender rod shows fluctuations and does not exhibit a linear correlation.

In summary, for midspan and arch crown dynamic displacements of the main beam, as well as the dynamic tension in the longest suspender rod, their dynamic amplification factors are negatively correlated with the number of lanes. Additionally, as the total applied load decreases, the decrease

in these factors also becomes less pronounced. On the other hand, for midspan dynamic moment of the main beam and dynamic tension in the shortest suspender rod, their dynamic amplification factors do not exhibit a linear correlation with the number of lanes. Finally, for arch crown dynamic moment, there is a positive correlation with the number of lanes.

4. Summary

(1) For the single-lane, single-vehicle vehicle-bridge coupled vibration response of the continuous rigid-frame bridge at a speed of 70 km/h, the dynamic response peak values of various cross-sections are observed.

(2) For multi-lane single-vehicle traffic in one direction, the vehicle-bridge coupled vibration response shows that as the number of lanes increases, the dynamic response peak values of various cross-sections increase. Specifically, when transitioning from a single-lane scenario to a double-lane scenario, the following changes were observed: The midspan dynamic displacement peak value of the main beam increased by 117%. The midspan dynamic bending moment peak value increased by 38.1%. The arch crown dynamic displacement peak value increased by 54%. The arch crown dynamic bending moment peak value increased by 41%. The dynamic tension peak value in the longest suspender rod increased by 59.7%. The dynamic tension peak value in the shortest suspender rod increased by 64.2%.

When transitioning from a double-lane scenario to a triple-lane scenario, the changes were as follows: The midspan dynamic displacement peak value of the main beam increased by 1.07%. The midspan dynamic bending moment peak value increased by 39.5%. The arch crown dynamic displacement peak value increased by 1.97%. The arch crown dynamic bending moment peak value increased by 21.80%. The dynamic tension peak value in the longest suspender rod increased by 1.16%. The dynamic tension peak value in the shortest suspender rod increased by 15.22%.

(3) Regarding the dynamic amplification factors, for the midspan and arch crown dynamic displacements and the dynamic tension in the longest suspender rods, these factors decrease as the number of lanes increases. Specifically, when transitioning from a single-lane scenario to a double-lane scenario: The dynamic amplification factor for midspan dynamic displacement of the main beam decreased by 12.92%. The dynamic amplification factor for arch crown dynamic displacement decreased by 15.95%.

When transitioning from a double-lane scenario to a triple-lane scenario: The dynamic amplification factor for midspan dynamic displacement of the main beam decreased by 0.97%. The dynamic amplification factor for arch crown dynamic displacement remained relatively stable, changing slightly from 1.499 to 1.502. For the dynamic bending moment amplification factors at the midspan and the dynamic tension amplification factors for the shortest suspender rods, there is no linear correlation with the number of lanes. However, for the dynamic bending moment amplification factor at the arch crown, there is a positive correlation with the number of lanes.

(4) For the continuous rigid-frame bridge system of the beam-arch combination, different components of the bridge have different dynamic amplification factors. The maximum dynamic amplification factors for various sections are as follows: midspan dynamic displacement of the main span (1.452), midspan dynamic bending moment (1.327), arch crown dynamic displacement (1.773), arch crown dynamic bending moment (3.137), dynamic tension in the longest suspender rod (1.602), and dynamic tension in the shortest suspender rod (1.265).

For this bridge, the specified dynamic amplification factor is 1.05. In comparison to the results of this study, the dynamic responses for various cross-sections exceed the specifications. Therefore, the current specifications for dynamic amplification factors for this type of bridge are considered

unsafe. Furthermore, using a unified maximum dynamic amplification factor for the entire bridge is inappropriate. Regarding the specification values for dynamic amplification factors, individual values should be assigned for each bridge component. In future designs, maintenance, and reinforcement of such bridges, these individual values should serve as references.

References

[1] Li Ximei, Xu Wei, Mu Bohai. Vehicle-Bridge Coupled Vertical Vibration Analysis of Steel-Concrete Composite Beam Bridges. Journal of Shenyang University of Technology, 2022, 44(02): 227-233.

[2] Bai Qi, Deng Nianchun. Analysis of Vehicle-Bridge Coupled Vibration Response for Long-Span Continuous Girder Bridge with Elastic Bearings. Journal of Shijiazhuang Tiedao University (Natural Science Edition), 2023, 36(01): 20-26.

[3] Han Zhiqiang, Xie Gang, Li Luyao, et al. Vehicle-Bridge Coupled Vibration Response of Long-Span Continuous Girder Bridge. Science, Technology and Engineering, 2022, 22(11): 4588-4595.

[4] Chen Zhaowei, Pu Qianhua. Suppression Characteristics of Elastic Wheels on Vehicle-Bridge Coupled Vibration of Long-Span Cable-Stayed Bridges. Journal of Jilin University (Engineering and Technology Edition), 2023.

[5] Ge Wei. Vehicle-Bridge Coupled Vibration Study of Multi-Tower Segmental Cable-Stayed Bridges. Chang'an University, 2021.

[6] He Xuanbo. Study on Corrosion Fatigue Characteristics of Short Hangers in a Mid-Span Supported Arch Bridge Considering Vehicle-Bridge Coupled Vibration. Chongqing Jiaotong University, 2022.

[7] Wang Xiaoyong, Wang Longlin, Zhang Lingling, et al. Analysis of Vehicle-Bridge Coupled Vibration Characteristics and Ride Comfort of a Continuous Rigid Frame Bridge. Western Transportation Science and Technology, 2022, 183(10): 150-153.

[8] Yao Dunrong, Deng Nianchun. Vehicle-Bridge Coupled Vibration Analysis of Long-Span Steel-Concrete Arch Bridge. Journal of Railway Science and Engineering, 2022, 19(12): 3693-3704.

[9] Sun, L, Zhao XZ. Coupled Dynamics of Vehicle-Bridge Interaction System Using High Efficiency Method. ADVANCES IN CIVIL ENGINEERING, 2021, 20, 1964200.1-1964200.22.

[10] Stoura, C. D., Paraskevopoulos, E., Dimitrakopoulos, E. G., & Natsiavas, S. A Dynamic Partitioning Method to solve the vehicle-bridge interaction problem. Computers & Structures, 2021, 251, 106547.

[11] Kim, J., Lynch, J. P. Experimental analysis of vehicle–bridge interaction using a wireless monitoring system and a two-stage system identification technique. Mechanical Systems and Signal Processing, 2012, 28, 3-19.

[12] Kim, J., Lynch, J. P., Lee, J. J., Lee, C. G. Truck-based mobile wireless sensor networks for the experimental observation of vehicle–bridge interaction. Smart Materials and Structures, 2011, 20(6), 065009.

[13] Liu Minghu. Engineering Practice and Prospects of Bridge Steel-Concrete Composite Technology. Bridge Construction, 2022, 52(01):18-25.